Am J Cancer Res 2025;15(5):2170-2179
www.ajcr.us /ISSN:2156-6976/ajcr0164698

Original Article

Identification of new natural compounds against KSHV-related malignancies

Jungang Chen*, Jiaojiao Fan*, Lu Dai, Zhiqiang Qin

*Department of Pathology, Winthrop P. Rockefeller Cancer Institute, University of Arkansas for Medical Sciences, 4301 W Markham St, Little Rock, AR 72205, USA. *Equal contributors.*

Received March 21, 2025; Accepted April 28, 2025; Epub May 15, 2025; Published May 30, 2025

Abstract: Kaposi's Sarcoma-associated Herpesvirus (KSHV) is the etiologic agent of several human cancers, including Kaposi's Sarcoma (KS) and Primary Effusion Lymphoma (PEL), which preferentially arise in immunocompromised patients and lack of effective therapeutic options. Increasing evidence has supported that many natural products from plants or other resources display anticancer activities, whereas only limited data reported them in the treatment of KSHV-related malignancies. In the current study, we identified 7 natural compounds displaying prominent anti-KS and anti-PEL activities after high-throughput screening of a natural compound library on TIVE-LTC and BCBL-1 cell lines, respectively. Remarkably, most of these compounds showed much less or no toxicity on normal cells. Some of these natural compounds effectively repress PEL expansion *in vivo*. RNA-Sequencing and functional validation assays revealed the anticancer mechanisms of these new compounds, and identified new cellular factors such as FN1 which is required for PEL survival and growth. Taken together, our study provides promising new directions for fighting these virus-associated malignancies.

Keywords: Drug screening, natural product, KSHV, KS, PEL

Introduction

Approximately 20% of human cancers have been attributed to viral infections, such as Kaposi's Sarcoma-associated Herpesvirus (KSHV, also named as Human Herpesvirus 8, HHV-8) [1]. Like other herpesviruses, KSHV can also establish lifetime infection in host cells. KSHV has two life-phases: a latent phase with a limited number of genes expressed and a lytic phase with most viral genes expressed that ultimately produces infectious virions [1]. In more than 90% of KSHV-infected host cells, the virus exists in the latency stage. However, no drugs are currently available to prevent KSHV infection, and current antiviral drugs are ineffective on viral latent infection. KSHV represents a principal causative agent of several cancers arising in patients with compromised immune systems, especially Kaposi's Sarcoma (KS) and Primary Effusion Lymphoma (PEL) [2, 3]. KS consist of spindle cells (the tumor cell with endothelial derivatives), a proliferation of abnormal and leaky vessels and extravasated red blood cells with hemosiderin deposits [2]. A prominent inflammatory infiltrate is also present early in the development of these lesions. Clinically, lesions have been described as patch, plaque, nodule and tumor stages, with individual patients often displaying different types of lesions. AIDS-associated KS (AIDS-KS) can present as an aggressive disseminated disease affecting skin, lymph nodes and visceral organs. Despite the reduced incidence of KS in the era of combined Antiretroviral Therapy (cART) for HIV infection, KS still remains the most common AIDS-associated tumor and a leading cause of morbidity and mortality in this setting [4, 5]. Further, a longitudinal study conducted among solid organ transplant recipients in US reported 15% of KSHV seropositivity in this population [6]. Transplant recipients who develop primary KSHV infection after transplantation have a relatively high probability of developing KSHV-related malignancies, especially KS [7], which is likely associated with the intensity of immunosuppressive treatment post-transplantation [8]. Another KSHV-caused ma-

lignancy, PEL, comprises transformed B cells harboring KSHV and arises preferentially within the pleural or peritoneal cavities of immunosuppressed patients [3]. PEL is a rapidly progressing malignancy with a median survival time of approximately 6 months, even under combinational chemotherapy [9]. Therefore, KSHV-induced malignancies still represent a serious threat to immunosuppressed patients due to the lack of effective therapies.

Currently, the combinational chemotherapy represents standard treatment of patients with KSHV-related malignancies. However, the myelosuppressive effects of systemic cytotoxic chemotherapy synergize with those caused by antiretroviral therapy or immune suppression [10, 11]. For example, the doxorubicin-induced cardiotoxicity has now become a serious threat to many cancer patients including KS or PEL patients [12-14]. Moreover, KSHV-infected tumor cells also have developed varied strategies for multidrug chemoresistance, discovered by us and other groups [15-17].

Increasing evidence has supported that many natural products from plants or other resources display anticancer activities, or enhance the efficacy of chemotherapy and other treatments while not affecting normal cells [18-20]. Additionally, many natural products display good antiviral activities as well. In contrast, there are few data reported natural products against KSHV-related malignancies especially the studies from high-throughput screening. In the current study, we identified 7 natural compounds displaying prominent anti-KS and anti-PEL activities after high-throughput screening of a Selleck compound library containing 756 natural compounds on TIVE-LTC and BCBL-1 cell lines, respectively. Remarkably, most of these compounds showed much less or no toxicity on normal cells. Some of these new natural compounds dramatically repressed PEL expansion in xenograft mice models. RNA-Sequencing and functional validation assays revealed the anticancer mechanisms of these new compounds, and identified new cellular factors such as Fibronectin 1 (FN1) which is required for PEL survival and growth. Taken together, our study provides promising new directions for fighting these virus-associated malignancies.

Materials and methods

Cell culture and reagents

BCBL-1 cells were kindly provided by Dr. Pinghui Feng (University of Southern California). KSHV long-term-infected telomerase-immortalized endothelial cells (TIVE-LTC) were kindly provided by Dr. Rolf Renne (University of Florida). Primary human umbilical vein endothelial cells (HUVEC) were purchased from American Type Culture Collection (ATCC), and cultured as recommended by the manufacturer. All experiments were carried out using cells harvested at low (< 20) passages. A compound library consisting of 756 natural products was purchased from Selleck Chemicals, USA.

High-throughput screening

BCBL-1 or TIVE-LTC (1×10^4 cells/well) were seeded into 96-well plates for 24 h, then the natural product compounds were added into the wells at a final concentration of 10 μM for an additional 72-h treatment. The cytotoxicity against tumor cells was measured using the WST-1 cell proliferation assays (Roche). Briefly, after the period of treatment of cells, 10 μL/well of cell proliferation reagent, WST-1 (4-[3-(4-Iodophenyl)-2-(4-nitro-phenyl)-2H-5-tetrazolio]-1,3-benzene disulfonate), was added and incubated for 3 h at 37°C in 5% CO_2. The absorbance of samples was measured by using a microplate reader at 490 nm. Data was normalized as the inhibition relative to the DMSO control.

Cell cycle assay

For cell cycle analysis, PEL cell pellets were fixed in 70% ethanol, and incubated at 4°C overnight. Cell pellets were re-suspended in 0.5 mL of 0.05 mg/mL PI plus 0.2 mg/mL RNaseA and incubated at 37°C for 30 min prior to FACS analysis.

Soft agar assays

Anchorage-independent growth of the tumor cells was assessed using soft agar assays. Briefly, a base layer containing 0.5% agar medium and 10% FBS was poured into six-well plates. Then, 2,000 cells were mixed with compounds and 0.35% agarose in medium containing 10% FBS to form a single-cell suspension.

After being seeded, the plates were incubated for 4-5 weeks. Colonies were stained with 0.005% crystal violet and photographed under a ChemiDoc Imaging system (Bio-Rad).

PEL xenograft models

NOD/SCID mice, 6-8-week old, male (Jackson Laboratory), 1 × 10^7 BCBL-1 cells in 200 µL RMPI-1640 without FBS were injected intraperitoneally (i.p.) and then mice were randomized into treatment groups of 6 mice as described previously [21]. Fangchinoline (25 mg/kg), Mycophenolic acid (25 mg/kg), 4'-Demethylpodophyllotoxin (20 mg/kg) or vehicle were administered i.p. initially at 48 h after BCBL-1 injections, twice a week for ~4 weeks. Weights were recorded weekly as a surrogate measure of tumor progression. All protocols were approved by the University of Arkansas for Medical Sciences Animal Care and Use Committee (No. 3960) in accordance with national guidelines.

RNA-sequencing and enrichment analysis

RNA-Sequencing of triplicate samples was performed by BGI Americas Corporation using their unique DNBSEQ™ sequencing technology. Raw sequencing reads were analyzed using the RSEM software (version 1.3.0; human GRCh38 genome sequence and annotation) and gene expression was quantified as previously described [22]. The EBSeq software was utilized to call differentially expressed genes that were statistically significant using a false discovery rate (FDR) less than 0.05. Differentially expressed genes between natural compounds- and vehicle-treated PEL cells were used as input for the GO_enrichment analyses.

RNA interference (RNAi)

For RNAi assays, FN1 On-Target plus SMARTpool small interfering RNA (siRNA; Dharmacon) or negative control siRNA were delivered using the DharmaFECT transfection reagent as recommended by the manufacturer.

Western blot

Total cell lysates (20 µg) were resolved by 10% SDS-PAGE, transferred to nitrocellulose membranes, and immunoblotted with antibodies to phosphor (p)-PI3K/total (t)-PI3K, p-Akt/t-Akt and Tubulin as a loading control (Cell Signaling). Immunoreactive bands were identified using an enhanced chemiluminescence reaction (Perkin-Elmer), and visualized by autoradiography.

RT-qPCR

Total RNA was isolated by using the RNeasy Mini kit (Qiagen), and cDNA was synthesized using a SuperScript III First-Strand Synthesis SuperMix Kit (Invitrogen). Specific primers used for amplification of individual target gene were listed in Table S1. The amplification was carried out using an iCycler IQ Real-Time PCR Detection System, and cycle threshold (Ct) values were tabulated in triplicate for each gene of interest in each experiment. "No template" (water) controls were used to ensure minimal background contamination. Using mean Ct values tabulated for each gene, and the paired Ct values for β-actin gene as a loading control, the fold changes for experimental groups relative to assigned control groups were calculated by using automated iQ5 2.0 software (Bio-rad).

Statistical analysis

Significant differences between experimental and control groups were determined using the two-tailed Student's *t*-test. The 50% Cytotoxicity Concentrations (CC_{50}) were calculated from the dose-response curves using GraphPad Prism 10.

Results

High-throughput screening and identification of new natural compounds displaying anti-PEL and anti-KS activities

Two KSHV+ tumor cell lines, BCBL-1 and TIVE-LTC, were used for our initial screening assays. After screening a chemical library containing 756 natural products, we found 36 (on BCBL-1) and 32 (on TIVE-LTC) compounds induced prominent cytotoxicity (> 60%) at 10 µM concentration (**Figure 1A**, **1B**). After searching published literature, we excluded those compounds with known anticancer activities. After calculating the 50% Cytotoxicity Concentrations (CC_{50}) using drug-killing curves on KSHV+ tumor cell lines and cross-analysis, we identified 15 compounds with CC_{50} < 5 µM on both BCBL-1 and TIVE-LTC (**Figure 1C**). After calculating selective index (SI, CC_{50} of HUVEC normal cells/CC_{50} of

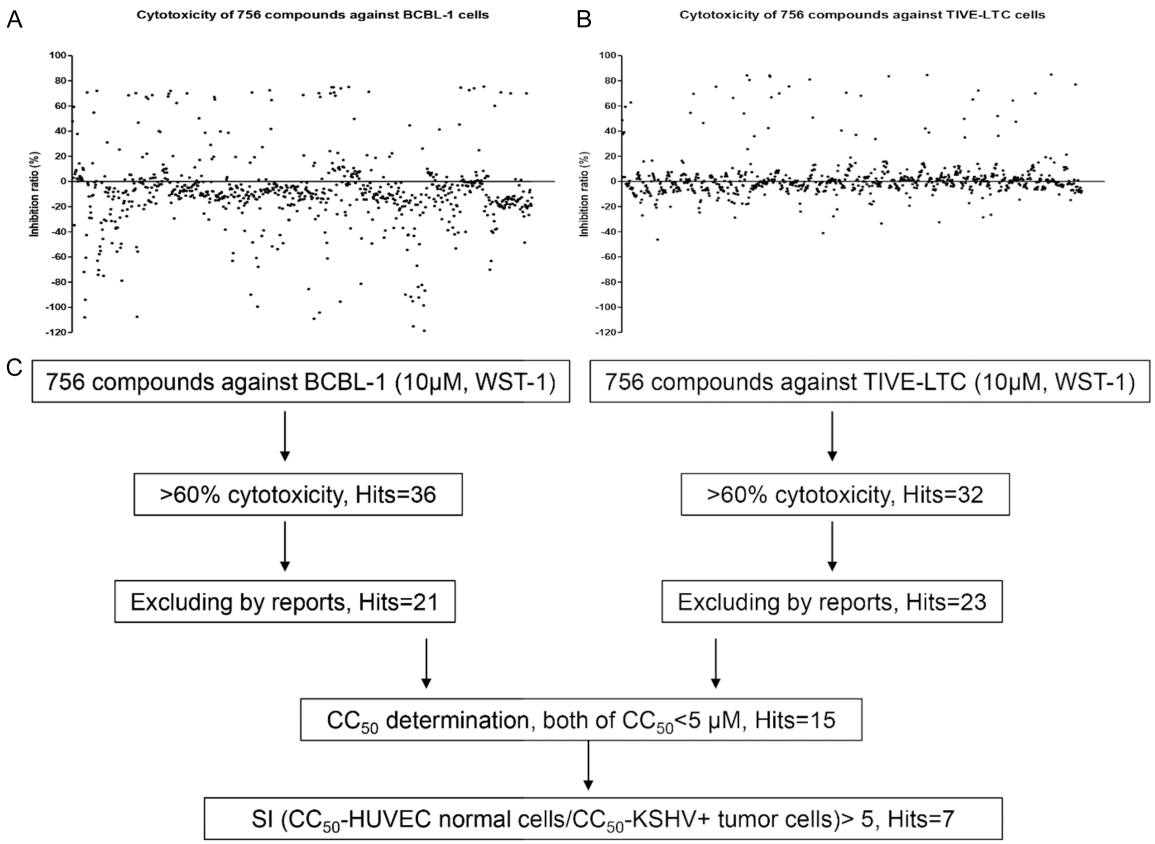

Figure 1. High-throughput screening and identification of new natural compounds against KSHV+ tumor cells. A and B. Primary screening results of 756 natural compounds against BCBL-1 or TIVE-LTC, which were arranged in order of inhibition rate. The natural compounds in source plates were delivered at 10 μM (final concentration) to 96-well plates seeded with BCBL-1 or TIVE-LTC for 72 h treatment, then cell proliferation was examined using the WST-1 cell proliferation assays (Roche). C. Diagrams of high-throughput drug screening and identification of final hits compounds.

Table 1. Final 7 hits natural compounds displaying effective anti-KSHV related malignancies activities

Compounds	CAS	CC_{50} (μM)[a]			Putative Targets
		BCBL-1	TIVE-LTC	HUVEC	
Mycophenolic acid	24280-93-1	0.2763	2.319	247	A potent IMPDH inhibitor used to prevent rejection in organ transplantation.
Combretastatin A4	117048-59-6	< 0.0046	< 0.0046	> 10	A microtubule-targeting agent that binds β-tubulin.
4'-Demethylpodophyllotoxin	40505-27-9	0.1093	0.1062	> 30	Unknown, remarkable cytotoxic potential in diverse cancer cell.
4'-Demethylepipodophyllotoxin	6559-91-7	1.5	0.195	> 30	A potent inhibitor of microtubule assembly.
Fangchinoline	33889-68-8	4.037	6.65	> 30	A HIV-1 inhibitor, inhibiting autophagosomes-lysosomes fusion and PI3K.
Protodioscin	55056-80-9	2.846	2.571	20	Targeting the testosterone receptors to induce testosterone production.
Chaetocin	28097-03-2	< 0.0046	< 0.0046	0.024	A histone methyltransferase inhibitor.

[a] CC_{50} represents the 50% cytotoxic concentration determined by the WST-1 cell proliferation assay (Roche).

KSHV+ tumor cells), we ultimately identified 7 hits compounds whose SI is above 5. These compounds include Mycophenolic acid, Combretastatin A4, 4'-Demethylepipodophyllotoxin, 4'-Demethylpodophyllotoxin, Fangchinoline, Protodioscin and Chaetocin. Notably, all of the 7 natural compounds showed low or no cytotoxicity on HUVEC, making them highly selective towards KSHV+ tumor cells and suitable for drug development (**Table 1**).

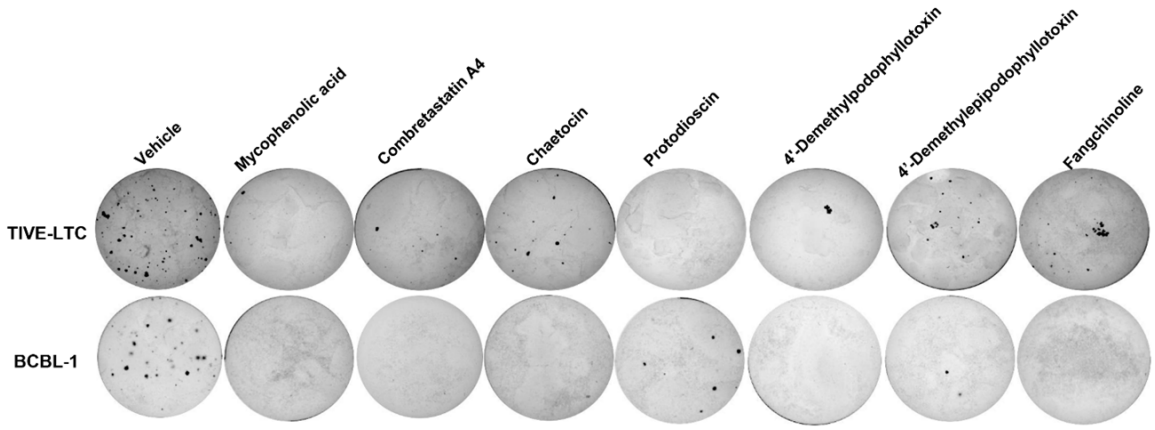

Figure 2. The new natural compounds effectively inhibit anchorage-independent growth of KSHV+ tumor cells. The inhibition of BCBL-1 and TIVE-LTC anchorage-independent growth by new natural compounds at their CC_{50} concentrations was tested using soft agar assays as described in Methods.

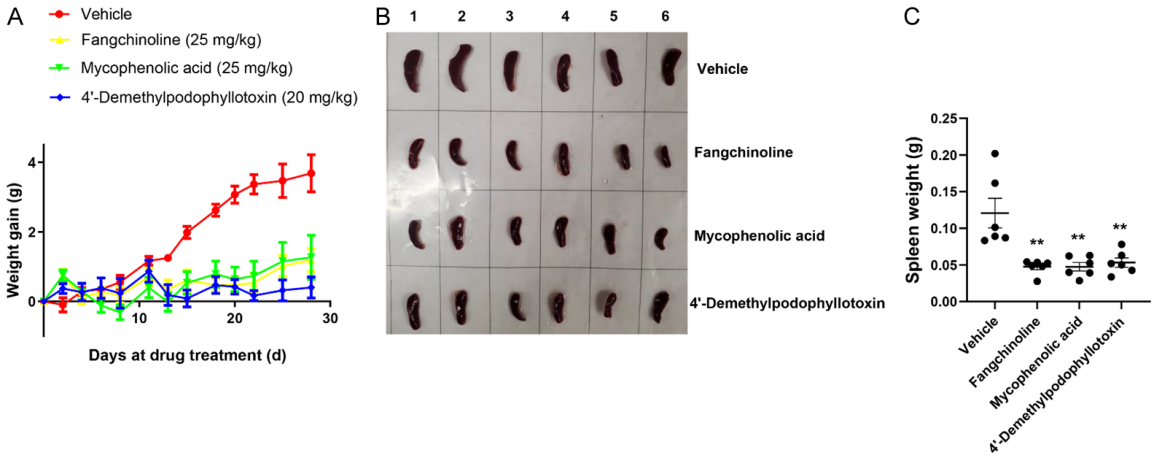

Figure 3. The new natural compounds treatments effectively repress PEL tumor progression *in vivo*. A. NOD/SCID mice (6 mice for each group) were injected i.p. with BCBL-1 cells. 48 h later, the Fangchinoline (25 mg/kg), Mycophenolic acid (25 mg/kg), 4'-Demethylpodophyllotoxin (20 mg/kg) or vehicle were administered i.p., twice a week for ~4 weeks, and weights were recorded weekly. B and C. At the end of the treatment period, the mice were sacrificed and spleens were collected for comparison. Error bars represent SEM for 6 mice from the same group, ** = P < 0.01 (*vs* the vehicle control).

By using the soft agar assays, we observed all of the 7 natural compounds treatments dramatically inhibited anchorage-independent growth of BCBL-1 and TIVE-LTC, respectively, at their CC_{50} concentrations. Compared to the vehicle control, these natural compounds treatments caused much smaller and fewer colony formation, some only having cell debris left after treatments (**Figure 2**).

The new natural compounds effectively repress PEL cell growth in vivo

To assess *in vivo* efficacy of our new natural compounds, we tested 3 of these compounds, Fangchinoline, Mycophenolic acid and 4'-Demethylpodophyllotoxin in an established PEL xenograft model wherein BCBL-1 cells were introduced into the peritoneal cavity of NOD/SCID mice [21]. We administered the natural compounds or vehicle i.p. within 48 hours of BCBL-1 injection and for about 4 weeks of treatment. All of the 3 natural compounds treatments dramatically suppressed PEL tumor progression over this timeframe when compared to the vehicle treated group (**Figure 3A**). The splenomegaly represents one of major indicators for lymphoma expansion in mice. After collecting spleens from sacrificed mice at the end of experiments, we found that all of the 3 natu-

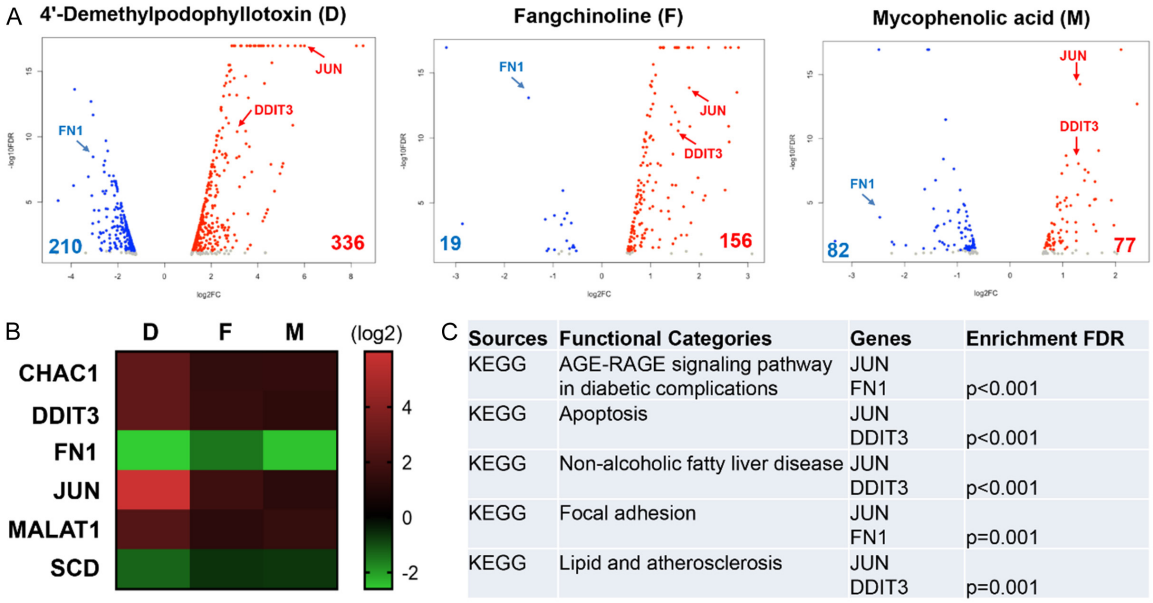

C

Sources	Functional Categories	Genes	Enrichment FDR
KEGG	AGE-RAGE signaling pathway in diabetic complications	JUN FN1	p<0.001
KEGG	Apoptosis	JUN DDIT3	p<0.001
KEGG	Non-alcoholic fatty liver disease	JUN DDIT3	p<0.001
KEGG	Focal adhesion	JUN FN1	p=0.001
KEGG	Lipid and atherosclerosis	JUN DDIT3	p=0.001

Figure 4. Transcriptome analysis of new natural compounds treated PEL cells. A. RNA-Sequencing was used to investigate changes in the transcriptome between natural compounds (Fangchinoline, Mycophenolic acid, 4'-Demethylpodophyllotoxin) and vehicle treated BCBL-1 cells. The significantly changed genes (FDR < 0.05) were shown in the Volcano plot panels. B and C. The heat maps showed commonly changed cellular genes by all of the 3 natural compounds in BCBL-1. Kyoto Encyclopedia of Genes and Genomes (KEGG) pathway analysis of commonly changed cellular genes in BCBL-1.

ral compounds treated mice had much smaller spleen than those vehicle treated mice (**Figure 3B**, **3C**). In addition, we almost do not observe ascites formation in all of the 3 natural compounds treated mice when compared to the vehicle treated group. These data together demonstrate satisfied *in vivo* efficacy of our new natural compounds against KSHV-related malignancies.

Transcriptomic analysis of gene profiling in PEL cells altered by new natural compounds

To determine the global cellular changes induced by these natural compounds, we compared the gene profiles of vehicle- to natural compound-treated BCBL-1 cells (Fangchinoline, Mycophenolic acid and 4'-Demethylpodophyllotoxin, respectively) by using RNA-Sequencing analyses. The volcano plots showed the scattering of genes which were significantly upregulated or downregulated (FDR < 0.05) in natural compounds treated BCBL-1: 156 upregulated and 19 downregulated by Fangchinoline; 77 upregulated and 82 downregulated by Mycophenolic acid; 336 upregulated and 210 downregulated by 4'-Demethylpodophyllotoxin (**Figure 4A** and Supplemental Data). After intersection analysis, the heat map indicated total 6 genes commonly changed (CHAC1, DDIT3, FN1, JUN, MALAT1, SCD) in BCBL-1 treated by all of the 3 natural compounds (**Figure 4B**). The Kyoto Encyclopedia of Genes and Genomes (KEGG) pathway analysis of these "common" genes indicated that the top 5 pathways were affected, especially the pathways about Apoptosis and Focal adhesion (**Figure 4C**), implying that these "common" genes may have close association with PEL cell survival and pathogenesis.

FN1 is required for the survival of KSHV+ tumor cells

We hypothesize that certain gene candidates (especially those changed by multiple natural compounds) identified from RNA-Sequencing analysis are potentially related to KSHV+ tumor cell survival and pathogenesis. Here we selected Fibronectin 1 (FN1), one of "common" genes downregulated by all of the 3 natural compounds for understanding its role in PEL cell survival. As a member of the FN family, FN1 is involved in a variety of cellular processes and in diseases such as cancer, arthritis and atherosclerosis [23]. Furthermore, one recent study

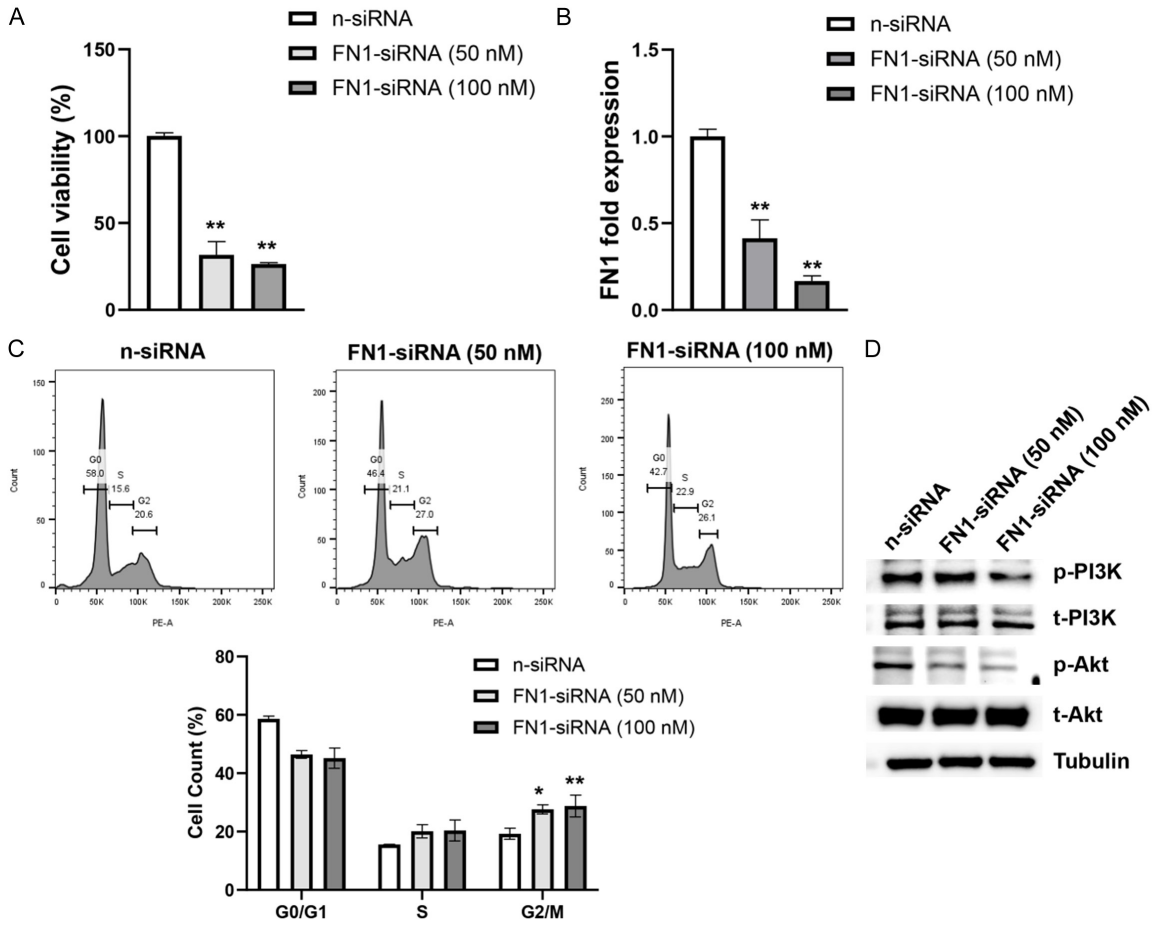

Figure 5. FN1 is required for the survival of KSHV+ tumor cells. A-D. BCBL-1 cells were transfected with *FN1*-siRNA or non-target control siRNA (n-siRNA) for 72 h, then the cell proliferation, gene transcription, cell cycle and protein expression were measured by using the WST-1 assays, RT-qPCR, flow cytometry and Western blot analysis, respectively. Error bars represent S.D. for 3 independent experiments, * = P < 0.05, ** = P < 0.01 (*vs* the n-siRNA control).

reported that silencing of the FN1 gene in human glioma cells inhibited cell proliferation, promoted cell apoptosis and senescence, and reduced cell migration and invasion through the disruption of the PI3K-Akt signaling pathway [24]. Our data demonstrated that direct knockdown of FN1 by RNAi dramatically reduced cell viability of BCBL-1 (**Figure 5A**, **5B**), through causing cell cycle arrest especially at G2/M phase (**Figure 5C**). To further explore the downstream signaling of FN1 in PEL cells, we found that silencing FN1 downregulated the activity of PI3K-Akt signaling (**Figure 5D**), which is closely related to PEL cell survival and proliferation [25]. Interestingly, we also found that silencing FN1 partially reduced viral latent gene (e.g., LANA) expression while increasing lytic gene (e.g., RTA, ORF59) expression from BCBL-1 cells (Figure S1).

Discussion

Currently, KSHV-related malignancies are still lacking of effective treatment options, while our data indicate that natural compounds may represent a promising strategy. Here we have identified 7 natural compounds displaying prominent anti-KS and anti-PEL activities after high-throughput screening of a natural compound library, which have never been reported before. Remarkably, most of these compounds show much less or no toxicity on normal cells. Three of them, Fangchinoline, Mycophenolic acid and 4'-Demethylpodophyllotoxin, also display satisfied efficacy in PEL xenograft models. One of these natural compounds, Fangchinoline, a bis-benzylisoquinoline alkaloid, has recently been reported with anticancer activities in hepatocellular carcinoma, through

reducing inflammation-induced epithelial-mesenchymal transition (EMT) while inducing reactive oxygen species (ROS) accumulation [26, 27]. Interestingly, another recent study has reported that Fangchinoline effectively impedes the replication of vesicular stomatitis virus (VSV), encephalomyocarditis virus (EMCV), influenza A virus (H1N1), and herpes simplex virus-1 (HSV-1) *in vitro* [28]. Mechanistically, Fangchinoline activates the antiviral response in a STING (stimulator of interferon genes)-dependent manner, leading to increased expression of interferon (IFN) and interferon-stimulated genes (ISGs) for potent antiviral effects. Therefore, we will examine whether Fangchinoline treatment may also affect KSHV replication in future study. Ma *et al* have identified six KSHV-encoded proteins that inhibit the cGMP-AMP synthase (cGAS)-STING DNA sensing pathway including viral interferon regulatory factor 1 (vIRF1), which targets STING by preventing it from interacting with TANK binding kinase 1 (TBK1), thereby inhibiting STING's phosphorylation and concomitant activation [29].

The other two natural compounds we tested *in vivo*, Mycophenolic acid and 4'-Demethylpodophyllotoxin, also have been tried in cancer treatment. For example, one recent study has reported that Mycophenolic acid and its synthesized analogues show potent anticancer activities on a panel of osteosarcoma cancer cell lines [30]. Another very recent study has found that 4'-Demethylpodophyllotoxin exhibits time- and dose-dependent growth inhibition on colorectal cancer cell lines and tumor organoids derived from patients, through targeting the PI3K-Akt pathway [31]. However, in the current study only three natural compounds were validated *in vivo*, so the clinical potential of the remaining natural compounds needs to be explored in future study.

By using RNA-Sequencing analyses, we have identified a subset of gene candidates which are commonly changed by multiple natural compounds in BCBL-1 cells. One of them, Metastasis associated lung adenocarcinoma transcript 1 (MALAT1), is upregulated in natural compounds treated BCBL-1 cells. As one of the first cancer-associated long non-coding RNAs (lncRNAs) discovered, the aberrant expression of MALAT1 has been found in different types of cancers [32]. Although most studies report that upregulation of MALAT1 is related to cancer cell malignant behaviors, there are a few studies report that MALAT1 can act as a tumor suppressor in some types of cancer. For example, overexpression of MALAT1 suppresses breast cancer metastasis in transgenic, xenograft, and syngeneic models, through inactivation of the prometastatic transcription factor TEAD, preventing TEAD from associating with its co-activator YAP and target gene promoters [33]. Han *et al* report that MALAT1 can suppress the invasion and proliferation of the glioma cells via downregulation of matrix metalloproteinase 2 (MMP2) and inactivation of mitogen-activated protein kinase/extracellular signal-regulated kinase (MAPK/ERK) signaling activities [34]. Therefore, we are interested to determine whether MALAT1 may have tumor-suppressive functions in KSHV+ tumor cells, too.

Another gene candidate, FN1, is downregulated in natural compounds treated BCBL-1 cells. However, the functions of FN1 in KSHV+ tumor cells remain almost unknown. Here we found that silencing FN1 reduced BCBL-1 cell viability but induced cell cycle arrest through downregulation of PI3K-Akt signaling activities. Interestingly, Ma *et al* have reported that FN1 overexpression is associated with EBV-encoded latent membrane protein 1 (LMP1) expression in tumor tissues, which has independent prognostic value for nasopharyngeal carcinoma (NPC), one of major EBV-related malignancies [35]. Therefore, future studies will focus on exploring FN1 immunoexpression status, and its associations with clinicopathological variables and survival in the cohort of patients with KSHV-related malignancies.

Acknowledgements

We thank Dr. Jovanny Zabaleta at Louisiana State University Health Sciences Center for help of RNA-Sequencing analysis. This work is supported by the Arkansas Bioscience Institute, the major research component of the Arkansas Tobacco Settlement Proceeds Act of 2000 and Arkansas Breast Cancer Research Program Pilot Award to Z.Q. L.D. was supported by a UAMS COM Pilot Award and a Winthrop P. Rockefeller Cancer Institute Seeds Award.

Disclosure of conflict of interest

None.

Address correspondence to: Zhiqiang Qin and Lu Dai, University of Arkansas for Medical Sciences, 4301 W Markham St, Little Rock, AR 72205, USA. Tel: 501-526-8619; E-mail: zqin@uams.edu (ZQQ); ldai@uams.edu (LD)

References

[1] Mesri EA, Feitelson MA and Munger K. Human viral oncogenesis: a cancer hallmarks analysis. Cell Host Microbe 2014; 15: 266-282.

[2] Chang Y, Cesarman E, Pessin MS, Lee F, Culpepper J, Knowles DM and Moore PS. Identification of herpesvirus-like DNA sequences in AIDS-associated Kaposi's sarcoma. Science 1994; 266: 1865-1869.

[3] Cesarman E, Chang Y, Moore PS, Said JW and Knowles DM. Kaposi's sarcoma-associated herpesvirus-like DNA sequences in AIDS-related body-cavity-based lymphomas. N Engl J Med 1995; 332: 1186-1191.

[4] Dupin N. Update on oncogenesis and therapy for Kaposi sarcoma. Curr Opin Oncol 2020; 32: 122-128.

[5] Dalla Pria A, Pinato DJ, Bracchi M and Bower M. Recent advances in HIV-associated Kaposi sarcoma. F1000Res 2019; 8: F1000 Faculty Rev-970.

[6] Jenkins FJ, Hoffman LJ and Liegey-Dougall A. Reactivation of and primary infection with human herpesvirus 8 among solid-organ transplant recipients. J Infect Dis 2002; 185: 1238-1243.

[7] Luppi M, Barozzi P, Santagostino G, Trovato R, Schulz TF, Marasca R, Bottalico D, Bignardi L and Torelli G. Molecular evidence of organ-related transmission of Kaposi sarcoma-associated herpesvirus or human herpesvirus-8 in transplant patients. Blood 2000; 96: 3279-3281.

[8] Ariza-Heredia EJ and Razonable RR. Human herpes virus 8 in solid organ transplantation. Transplantation 2011; 92: 837-844.

[9] Okada S, Goto H and Yotsumoto M. Current status of treatment for primary effusion lymphoma. Intractable Rare Dis Res 2014; 3: 65-74.

[10] Simonelli C, Spina M, Cinelli R, Talamini R, Tedeschi R, Gloghini A, Vaccher E, Carbone A and Tirelli U. Clinical features and outcome of primary effusion lymphoma in HIV-infected patients: a single-institution study. J Clin Oncol 2003; 21: 3948-3954.

[11] Boulanger E, Gerard L, Gabarre J, Molina JM, Rapp C, Abino JF, Cadranel J, Chevret S and Oksenhendler E. Prognostic factors and outcome of human herpesvirus 8-associated primary effusion lymphoma in patients with AIDS. J Clin Oncol 2005; 23: 4372-4380.

[12] Argun M, Uzum K, Sonmez MF, Ozyurt A, Derya K, Cilenk KT, Unalmis S, Pamukcu O, Baykan A, Narin F, Elmali F and Narin N. Cardioprotective effect of metformin against doxorubicin cardiotoxicity in rats. Anatol J Cardiol 2016; 16: 234-241.

[13] McGowan JV, Chung R, Maulik A, Piotrowska I, Walker JM and Yellon DM. Anthracycline chemotherapy and cardiotoxicity. Cardiovasc Drugs Ther 2017; 31: 63-75.

[14] Bahadir A, Kurucu N, Kadioglu M and Yenilme E. The role of nitric oxide in Doxorubicin-induced cardiotoxicity: experimental study. Turk J Haematol 2014; 31: 68-74.

[15] Qin Z, Dai L, Bratoeva M, Slomiany MG, Toole BP and Parsons C. Cooperative roles for emmprin and LYVE-1 in the regulation of chemoresistance for primary effusion lymphoma. Leukemia 2011; 25: 1598-1609.

[16] Otvos R, Skribek H, Kis LL, Gloghini A, Markasz L, Flaberg E, Eksborg S, Konya J, Gergely L, Carbone A and Szekely L. Drug sensitivity patterns of HHV8 carrying body cavity lymphoma cell lines. BMC Cancer 2011; 11: 441.

[17] Chen J, Kendrick S and Qin Z. Mechanistic insights into chemoresistance mediated by oncogenic viruses in lymphomas. Viruses 2019; 11: 1161.

[18] Subramaniam S, Selvaduray KR and Radhakrishnan AK. Bioactive compounds: natural defense against cancer? Biomolecules 2019; 9: 758.

[19] Cullen JK, Simmons JL, Parsons PG and Boyle GM. Topical treatments for skin cancer. Adv Drug Deliv Rev 2020; 153: 54-64.

[20] Muniraj N, Siddharth S and Sharma D. Bioactive compounds: multi-targeting silver bullets for preventing and treating breast cancer. Cancers (Basel) 2019; 11: 1563.

[21] Dai L, Trillo-Tinoco J, Cao Y, Bonstaff K, Doyle L, Del Valle L, Whitby D, Parsons C, Reiss K, Zabaleta J and Qin Z. Targeting HGF/c-MET induces cell cycle arrest, DNA damage, and apoptosis for primary effusion lymphoma. Blood 2015; 126: 2821-2831.

[22] Kheir F, Zhao M, Strong MJ, Yu Y, Nanbo A, Flemington EK, Morris GF, Reiss K, Li L and Lin Z. Detection of Epstein-Barr virus infection in non-small cell lung cancer. Cancers (Basel) 2019; 11: 759.

[23] Goossens K, Van Soom A, Van Zeveren A, Favoreel H and Peelman LJ. Quantification of fibronectin 1 (FN1) splice variants, including two novel ones, and analysis of integrins as candidate FN1 receptors in bovine preimplantation embryos. BMC Dev Biol 2009; 9: 1.

[24] Liao YX, Zhang ZP, Zhao J and Liu JP. Effects of fibronectin 1 on cell proliferation, senescence and apoptosis of human glioma cells through

the PI3K/AKT signaling pathway. Cell Physiol Biochem 2018; 48: 1382-1396.
[25] Bhatt AP and Damania B. AKTivation of PI3K/AKT/mTOR signaling pathway by KSHV. Front Immunol 2013; 3: 401.
[26] Zheng L, Rajamanickam V, Wang M, Zhang H, Fang S, Linnebacher M, Abd El-Aty AM, Zhang X, Zhang Y, Wang J, Chen M, Zhao Z and Ji J. Fangchinoline inhibits metastasis and reduces inflammation-induced epithelial-mesenchymal transition by targeting the FOXM1-ADAM17 axis in hepatocellular carcinoma. Cell Signal 2024; 124: 111467.
[27] Liu Y, Wang Y, Wang J, Wang X, Chen L, Han T, Lian H, Gan M and Wang J. Fangchinoline suppresses hepatocellular carcinoma by regulating ROS accumulation via the TRIM7/Nrf2 signaling pathway. Phytomedicine 2024; 135: 156143.
[28] Wang J, Xie F, Jia X, Wang X, Kong L, Li Y, Liang X, Zhang M, He Y, Feng W, Luo T, Wang Y and Xu A. Fangchinoline induces antiviral response by suppressing STING degradation. J Pharm Anal 2024; 14: 100972.
[29] Ma Z, Jacobs SR, West JA, Stopford C, Zhang Z, Davis Z, Barber GN, Glaunsinger BA, Dittmer DP and Damania B. Modulation of the cGAS-STING DNA sensing pathway by gammaherpesviruses. Proc Natl Acad Sci U S A 2015; 112: E4306-4315.
[30] Silalai P, Teeyakasem P, Pruksakorn D and Saeeng R. Design and synthesis of mycophenolic acid analogues for osteosarcoma cancer treatment. ACS Bio Med Chem Au 2024; 5: 106-118.
[31] Liu J, Luo D, Chen X, Liu J, Chen J, Shi M, Dong H, Xu Y, Wang X, Yu Z, Liu H and Feng Y. 4'-Demethylpodophyllotoxin functions as a mechanism-driven therapy by targeting the PI3K-AKT pathway in Colorectal cancer. Transl Oncol 2025; 51: 102199.
[32] Amodio N, Raimondi L, Juli G, Stamato MA, Caracciolo D, Tagliaferri P and Tassone P. MALAT1: a druggable long non-coding RNA for targeted anti-cancer approaches. J Hematol Oncol 2018; 11: 63.
[33] Kim J, Piao HL, Kim BJ, Yao F, Han Z, Wang Y, Xiao Z, Siverly AN, Lawhon SE, Ton BN, Lee H, Zhou Z, Gan B, Nakagawa S, Ellis MJ, Liang H, Hung MC, You MJ, Sun Y and Ma L. Long noncoding RNA MALAT1 suppresses breast cancer metastasis. Nat Genet 2018; 50: 1705-1715.
[34] Han Y, Wu Z, Wu T, Huang Y, Cheng Z, Li X, Sun T, Xie X, Zhou Y and Du Z. Tumor-suppressive function of long noncoding RNA MALAT1 in glioma cells by downregulation of MMP2 and inactivation of ERK/MAPK signaling. Cell Death Dis 2016; 7: e2123.
[35] Ma LJ, Lee SW, Lin LC, Chen TJ, Chang IW, Hsu HP, Chang KY, Huang HY and Li CF. Fibronectin overexpression is associated with latent membrane protein 1 expression and has independent prognostic value for nasopharyngeal carcinoma. Tumour Biol 2014; 35: 1703-1712.

Table S1. Primer sequences for RT-qPCR

Gene	Sequences (5'→3')
LANA	*Sense TCCCTCTACACTAAACCCAATA*
	Antisense TTGCTAATCTCGTTGTCCC
RTA	*Sense CACAAAAATGGCGCAAGATGA*
	Antisense TGGTAGAGTTGGGCCTTCAGTT
ORF59	*Sense CGAGTCTTCGCAAAAGGTTC*
	Antisense AAGGGACCAACTGGTGTGAG
FN1	*Sense ACAGGACGGACATCTTTG*
	Antisense TTCTGGTCGGCATCATAG
β-actin	*Sense GGAAATCGTGCGTGACATT*
	Antisense GACTCGTCATACTCCTGCTTG

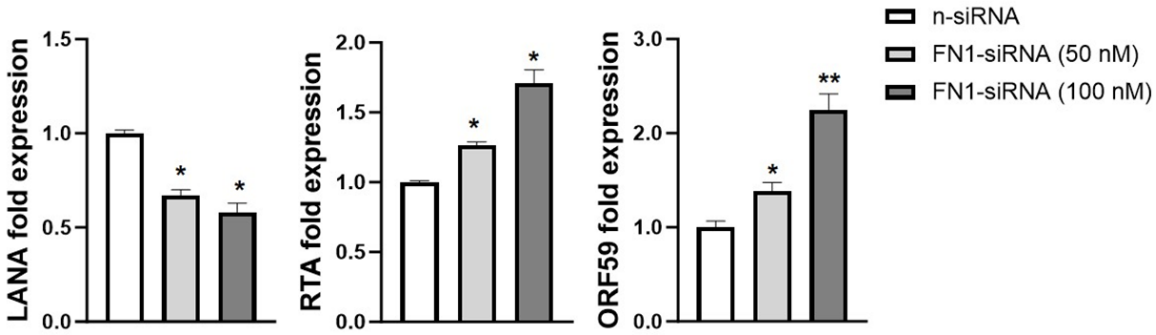

Figure S1. Targeting FN1 affects viral gene expression in KSHV+ tumor cells. BCBL-1 cells were transfected with *FN1*-siRNA or non-target control siRNA (n-siRNA) for 72 h, then viral gene transcription was measured and quantified by using the RT-qPCR assay. Error bars represent S.D. for 3 independent experiments, * = P < 0.05, ** = P < 0.01 (*vs* the n-siRNA control).